# Measurement of Semileptonic Branching Fractions of *B* Mesons to Narrow *D*** States

V. M. Abazov,[35] B. Abbott,[72] M. Abolins,[63] B. S. Acharya,[29] M. Adams,[50] T. Adams,[48] M. Agelou,[18] J.-L. Agram,[19] S. H. Ahn,[31] M. Ahsan,[57] G. D. Alexeev,[35] G. Alkhazov,[39] A. Alton,[62] G. Alverson,[61] G. A. Alves,[2] M. Anastasoaie,[34] T. Andeen,[52] S. Anderson,[44] B. Andrieu,[17] Y. Arnoud,[14] A. Askew,[48] B. Åsman,[40] A. C. S. Assis Jesus,[3] O. Atramentov,[55] C. Autermann,[21] C. Avila,[8] F. Badaud,[13] A. Baden,[59] L. Bagby,[51] B. Baldin,[49] P. W. Balm,[33] P. Banerjee,[29] S. Banerjee,[29] E. Barberis,[61] P. Bargassa,[76] P. Baringer,[56] C. Barnes,[42] J. Barreto,[2] J. F. Bartlett,[49] U. Bassler,[17] D. Bauer,[53] A. Bean,[56] S. Beauceron,[17] M. Begalli,[3] M. Begel,[68] A. Bellavance,[65] S. B. Beri,[27] G. Bernardi,[17] R. Bernhard,[49,*] I. Bertram,[41] M. Besançon,[18] R. Beuselinck,[42] V. A. Bezzubov,[38] P. C. Bhat,[49] V. Bhatnagar,[27] M. Binder,[25] C. Biscarat,[41] K. M. Black,[60] I. Blackler,[42] G. Blazey,[51] F. Blekman,[42] S. Blessing,[48] D. Bloch,[19] U. Blumenschein,[23] A. Boehnlein,[49] O. Boeriu,[54] T. A. Bolton,[57] F. Borcherding,[49] G. Borissov,[41] K. Bos,[33] T. Bose,[67] A. Brandt,[74] R. Brock,[63] G. Brooijmans,[67] A. Bross,[49] N. J. Buchanan,[48] D. Buchholz,[52] M. Buehler,[50] V. Buescher,[23] S. Burdin,[49] S. Burke,[44] T. H. Burnett,[78] E. Busato,[17] C. P. Buszello,[42] J. M. Butler,[60] J. Cammin,[68] S. Caron,[33] W. Carvalho,[3] B. C. K. Casey,[73] N. M. Cason,[54] H. Castilla-Valdez,[32] S. Chakrabarti,[29] D. Chakraborty,[51] K. M. Chan,[68] A. Chandra,[29] D. Chapin,[73] F. Charles,[19] E. Cheu,[44] D. K. Cho,[60] S. Choi,[47] B. Choudhary,[28] T. Christiansen,[25] L. Christofek,[56] D. Claes,[65] B. Clément,[19] C. Clément,[40] Y. Coadou,[5] M. Cooke,[76] W. E. Cooper,[49] D. Coppage,[56] M. Corcoran,[76] A. Cothenet,[15] M.-C. Cousinou,[15] B. Cox,[43] S. Crépé-Renaudin,[14] D. Cutts,[73] H. da Motta,[2] M. Das,[58] B. Davies,[41] G. Davies,[42] G. A. Davis,[52] K. De,[74] P. de Jong,[33] S. J. de Jong,[34] E. De La Cruz-Burelo,[62] C. De Oliveira Martins,[3] S. Dean,[43] J. D. Degenhardt,[62] F. Déliot,[18] M. Demarteau,[49] R. Demina,[68] P. Demine,[18] D. Denisov,[49] S. P. Denisov,[38] S. Desai,[69] H. T. Diehl,[49] M. Diesburg,[49] M. Doidge,[41] H. Dong,[69] S. Doulas,[61] L. V. Dudko,[37] L. Duflot,[16] S. R. Dugad,[29] A. Duperrin,[15] J. Dyer,[63] A. Dyshkant,[51] M. Eads,[51] D. Edmunds,[63] T. Edwards,[43] J. Ellison,[47] J. Elmsheuser,[25] V. D. Elvira,[49] S. Eno,[59] P. Ermolov,[37] O. V. Eroshin,[38] J. Estrada,[49] H. Evans,[67] A. Evdokimov,[36] V. N. Evdokimov,[38] J. Fast,[49] S. N. Fatakia,[60] L. Feligioni,[60] A. V. Ferapontov,[38] T. Ferbel,[68] F. Fiedler,[25] F. Filthaut,[34] W. Fisher,[49] H. E. Fisk,[49] I. Fleck,[23] M. Fortner,[51] H. Fox,[23] S. Fu,[49] S. Fuess,[49] T. Gadfort,[78] C. F. Galea,[34] E. Gallas,[49] E. Galyaev,[54] C. Garcia,[68] A. Garcia-Bellido,[78] J. Gardner,[56] V. Gavrilov,[36] A. Gay,[19] P. Gay,[13] D. Gelé,[19] R. Gelhaus,[47] K. Genser,[49] C. E. Gerber,[50] Y. Gershtein,[48] D. Gillberg,[5] G. Ginther,[68] T. Golling,[22] N. Gollub,[40] B. Gómez,[8] K. Gounder,[49] A. Goussiou,[54] P. D. Grannis,[69] S. Greder,[3] H. Greenlee,[49] Z. D. Greenwood,[58] E. M. Gregores,[4] Ph. Gris,[13] J.-F. Grivaz,[16] L. Groer,[67] S. Grünendahl,[49] M. W. Grünewald,[30] S. N. Gurzhiev,[38] G. Gutierrez,[49] P. Gutierrez,[72] A. Haas,[67] N. J. Hadley,[59] S. Hagopian,[48] I. Hall,[72] R. E. Hall,[46] C. Han,[62] L. Han,[7] K. Hanagaki,[49] K. Harder,[57] A. Harel,[26] R. Harrington,[61] J. M. Hauptman,[55] R. Hauser,[63] J. Hays,[52] T. Hebbeker,[21] D. Hedin,[51] J. M. Heinmiller,[50] A. P. Heinson,[47] U. Heintz,[60] C. Hensel,[56] G. Hesketh,[61] M. D. Hildreth,[54] R. Hirosky,[77] J. D. Hobbs,[69] B. Hoeneisen,[12] M. Hohlfeld,[24] S. J. Hong,[31] R. Hooper,[73] P. Houben,[33] Y. Hu,[69] J. Huang,[53] V. Hynek,[9] I. Iashvili,[47] R. Illingworth,[49] A. S. Ito,[49] S. Jabeen,[56] M. Jaffré,[16] S. Jain,[72] V. Jain,[70] K. Jakobs,[23] A. Jenkins,[42] R. Jesik,[42] K. Johns,[44] M. Johnson,[49] A. Jonckheere,[49] P. Jonsson,[42] A. Juste,[49] D. Käfer,[21] S. Kahn,[70] E. Kajfasz,[15] A. M. Kalinin,[35] J. Kalk,[63] D. Karmanov,[37] J. Kasper,[60] D. Kau,[48] R. Kaur,[27] R. Kehoe,[75] S. Kermiche,[15] S. Kesisoglou,[73] A. Khanov,[68] A. Kharchilava,[54] Y. M. Kharzheev,[35] H. Kim,[74] T. J. Kim,[31] B. Klima,[49] J. M. Kohli,[27] J.-P. Konrath,[23] M. Kopal,[72] V. M. Korablev,[38] J. Kotcher,[70] B. Kothari,[67] A. Koubarovsky,[37] A. V. Kozelov,[38] J. Kozminski,[63] A. Kryemadhi,[77] S. Krzywdzinski,[49] Y. Kulik,[49] A. Kumar,[28] S. Kunori,[59] A. Kupco,[11] T. Kurča,[20] J. Kvita,[9] S. Lager,[40] N. Lahrichi,[18] G. Landsberg,[73] J. Lazoflores,[48] A.-C. Le Bihan,[19] P. Lebrun,[20] W. M. Lee,[48] A. Leflat,[37] F. Lehner,[49,*] C. Leonidopoulos,[67] J. Leveque,[44] P. Lewis,[42] J. Li,[74] Q. Z. Li,[49] J. G. R. Lima,[51] D. Lincoln,[49] S. L. Linn,[48] J. Linnemann,[63] V. V. Lipaev,[38] R. Lipton,[49] L. Lobo,[42] A. Lobodenko,[39] M. Lokajicek,[11] A. Lounis,[19] P. Love,[41] H. J. Lubatti,[78] L. Lueking,[49] M. Lynker,[54] A. L. Lyon,[49] A. K. A. Maciel,[51] R. J. Madaras,[45] P. Mättig,[26] C. Magass,[21] A. Magerkurth,[62] A.-M. Magnan,[14] N. Makovec,[16] P. K. Mal,[29] H. B. Malbouisson,[3] S. Malik,[65] V. L. Malyshev,[35] H. S. Mao,[6] Y. Maravin,[49] M. Martens,[49] S. E. K. Mattingly,[73] A. A. Mayorov,[38] R. McCarthy,[69] R. McCroskey,[44] D. Meder,[24] A. Melnitchouk,[64] A. Mendes,[15] M. Merkin,[37] K. W. Merritt,[49] A. Meyer,[21] J. Meyer,[22] M. Michaut,[18] H. Miettinen,[76] J. Mitrevski,[67] J. Molina,[3] N. K. Mondal,[29] R. W. Moore,[5] T. Moulik,[56] G. S. Muanza,[20] M. Mulders,[49] L. Mundim,[3] Y. D. Mutaf,[69] E. Nagy,[15] M. Narain,[60] N. A. Naumann,[34] H. A. Neal,[62] J. P. Negret,[8] S. Nelson,[48] P. Neustroev,[39] C. Noeding,[23] A. Nomerotski,[49] S. F. Novaes,[4] T. Nunnemann,[25] E. Nurse,[43] V. O'Dell,[49] D. C. O'Neil,[5] V. Oguri,[3] N. Oliveira,[3] N. Oshima,[49] G. J. Otero y Garzón,[50] P. Padley,[76] N. Parashar,[58] S. K. Park,[31] J. Parsons,[67] R. Partridge,[73] N. Parua,[69] A. Patwa,[70] G. Pawloski,[76] P. M. Perea,[47] E. Perez,[18] P. Pétroff,[16] M. Petteni,[42] R. Piegaia,[1] M.-A. Pleier,[68] P. L. M. Podesta-Lerma,[32] V. M. Podstavkov,[49] Y. Pogorelov,[54] M.-E. Pol,[2] A. Pompoš,[72]

B. G. Pope,[63] W. L. Prado da Silva,[3] H. B. Prosper,[48] S. Protopopescu,[70] J. Qian,[62] A. Quadt,[22] B. Quinn,[64] K. J. Rani,[29] K. Ranjan,[28] P. A. Rapidis,[49] P. N. Ratoff,[41] S. Reucroft,[61] M. Rijssenbeek,[69] I. Ripp-Baudot,[19] F. Rizatdinova,[57] S. Robinson,[42] R. F. Rodrigues,[3] C. Royon,[18] P. Rubinov,[49] R. Ruchti,[54] V. I. Rud,[37] G. Sajot,[14] A. Sánchez-Hernández,[32] M. P. Sanders,[59] A. Santoro,[3] G. Savage,[49] L. Sawyer,[58] T. Scanlon,[42] D. Schaile,[25] R. D. Schamberger,[69] Y. Scheglov,[39] H. Schellman,[52] P. Schieferdecker,[25] C. Schmitt,[26] C. Schwanenberger,[22] A. Schwartzman,[66] R. Schwienhorst,[63] S. Sengupta,[48] H. Severini,[72] E. Shabalina,[50] M. Shamim,[57] V. Shary,[18] A. A. Shchukin,[38] W. D. Shephard,[54] R. K. Shivpuri,[28] D. Shpakov,[61] R. A. Sidwell,[57] V. Simak,[10] V. Sirotenko,[49] P. Skubic,[72] P. Slattery,[68] R. P. Smith,[49] K. Smolek,[10] G. R. Snow,[65] J. Snow,[71] S. Snyder,[70] S. Söldner-Rembold,[43] X. Song,[51] L. Sonnenschein,[17] A. Sopczak,[41] M. Sosebee,[74] K. Soustruznik,[9] M. Souza,[2] B. Spurlock,[74] N. R. Stanton,[57] J. Stark,[14] J. Steele,[58] K. Stevenson,[53] V. Stolin,[36] A. Stone,[50] D. A. Stoyanova,[38] J. Strandberg,[40] M. A. Strang,[74] M. Strauss,[72] R. Ströhmer,[25] D. Strom,[52] M. Strovink,[45] L. Stutte,[49] S. Sumowidagdo,[48] A. Sznajder,[3] M. Talby,[15] P. Tamburello,[44] W. Taylor,[5] P. Telford,[43] J. Temple,[44] M. Titov,[23] M. Tomoto,[49] T. Toole,[59] J. Torborg,[54] S. Towers,[69] T. Trefzger,[24] S. Trincaz-Duvoid,[17] D. Tsybychev,[69] B. Tuchming,[18] C. Tully,[66] A. S. Turcot,[43] P. M. Tuts,[67] L. Uvarov,[39] S. Uvarov,[39] S. Uzunyan,[51] B. Vachon,[5] P. J. van den Berg,[33] R. Van Kooten,[53] W. M. van Leeuwen,[33] N. Varelas,[50] E. W. Varnes,[44] A. Vartapetian,[74] I. A. Vasilyev,[38] M. Vaupel,[26] P. Verdier,[20] L. S. Vertogradov,[35] M. Verzocchi,[59] F. Villeneuve-Seguier,[42] J.-R. Vlimant,[17] E. Von Toerne,[57] M. Vreeswijk,[33] T. Vu Anh,[16] H. D. Wahl,[48] L. Wang,[59] J. Warchol,[54] G. Watts,[78] M. Wayne,[54] M. Weber,[49] H. Weerts,[63] N. Wermes,[22] M. Wetstein,[59] A. White,[74] V. White,[49] D. Wicke,[49] D. A. Wijngaarden,[34] G. W. Wilson,[56] S. J. Wimpenny,[47] J. Wittlin,[60] M. Wobisch,[49] J. Womersley,[49] D. R. Wood,[61] T. R. Wyatt,[43] Q. Xu,[62] N. Xuan,[54] S. Yacoob,[52] R. Yamada,[49] M. Yan,[59] T. Yasuda,[49] Y. A. Yatsunenko,[35] Y. Yen,[26] K. Yip,[70] H. D. Yoo,[73] S. W. Youn,[52] J. Yu,[74] A. Yurkewicz,[69] A. Zabi,[16] A. Zatserklyaniy,[51] M. Zdrazil,[69] C. Zeitnitz,[24] D. Zhang,[49] X. Zhang,[72] T. Zhao,[78] Z. Zhao,[62] B. Zhou,[62] J. Zhu,[69] M. Zielinski,[68] D. Zieminska,[53] A. Zieminski,[53] R. Zitoun,[69] V. Zutshi,[51] and E. G. Zverev[37]

(D0 Collaboration)

[1]*Universidad de Buenos Aires, Buenos Aires, Argentina*
[2]*LAFEX, Centro Brasileiro de Pesquisas Físicas, Rio de Janeiro, Brazil*
[3]*Universidade do Estado do Rio de Janeiro, Rio de Janeiro, Brazil*
[4]*Instituto de Física Teórica, Universidade Estadual Paulista, São Paulo, Brazil*
[5]*University of Alberta, Edmonton, Alberta, Canada, Simon Fraser University, Burnaby, British Columbia, Canada, York University, Toronto, Ontario, Canada, and McGill University, Montreal, Quebec, Canada*
[6]*Institute of High Energy Physics, Beijing, People's Republic of China*
[7]*University of Science and Technology of China, Hefei, People's Republic of China*
[8]*Universidad de los Andes, Bogotá, Colombia*
[9]*Center for Particle Physics, Charles University, Prague, Czech Republic*
[10]*Czech Technical University, Prague, Czech Republic*
[11]*Center for Particle Physics, Institute of Physics, Academy of Sciences of the Czech Republic, Prague, Czech Republic*
[12]*Universidad San Francisco de Quito, Quito, Ecuador*
[13]*Laboratoire de Physique Corpusculaire, IN2P3-CNRS, Université Blaise Pascal, Clermont-Ferrand, France*
[14]*Laboratoire de Physique Subatomique et de Cosmologie, IN2P3-CNRS, Universite de Grenoble 1, Grenoble, France*
[15]*CPPM, IN2P3-CNRS, Université de la Méditerranée, Marseille, France*
[16]*IN2P3-CNRS, Laboratoire de l'Accélérateur Linéaire, Orsay, France*
[17]*LPNHE, IN2P3-CNRS, Universités Paris VI and VII, Paris, France*
[18]*DAPNIA/Service de Physique des Particules, CEA, Saclay, France*
[19]*IReS, IN2P3-CNRS, Université Louis Pasteur, Strasbourg, France, and Université de Haute Alsace, Mulhouse, France*
[20]*Institut de Physique Nucléaire de Lyon, IN2P3-CNRS, Université Claude Bernard, Villeurbanne, France*
[21]*III. Physikalisches Institut A, RWTH Aachen, Aachen, Germany*
[22]*Physikalisches Institut, Universität Bonn, Bonn, Germany*
[23]*Physikalisches Institut, Universität Freiburg, Freiburg, Germany*
[24]*Institut für Physik, Universität Mainz, Mainz, Germany*
[25]*Ludwig-Maximilians-Universität München, München, Germany*
[26]*Fachbereich Physik, University of Wuppertal, Wuppertal, Germany*
[27]*Panjab University, Chandigarh, India*
[28]*Delhi University, Delhi, India*
[29]*Tata Institute of Fundamental Research, Mumbai, India*
[30]*University College Dublin, Dublin, Ireland*

[31]*Korea Detector Laboratory, Korea University, Seoul, Korea*
[32]*CINVESTAV, Mexico City, Mexico*
[33]*FOM-Institute NIKHEF and University of Amsterdam/NIKHEF, Amsterdam, The Netherlands*
[34]*Radboud University Nijmegen/NIKHEF, Nijmegen, The Netherlands*
[35]*Joint Institute for Nuclear Research, Dubna, Russia*
[36]*Institute for Theoretical and Experimental Physics, Moscow, Russia*
[37]*Moscow State University, Moscow, Russia*
[38]*Institute for High Energy Physics, Protvino, Russia*
[39]*Petersburg Nuclear Physics Institute, St. Petersburg, Russia*
[40]*Lund University, Lund, Sweden, Royal Institute of Technology and Stockholm University, Stockholm, Sweden,
and Uppsala University, Uppsala, Sweden*
[41]*Lancaster University, Lancaster, United Kingdom*
[42]*Imperial College, London, United Kingdom*
[43]*University of Manchester, Manchester, United Kingdom*
[44]*University of Arizona, Tucson, Arizona 85721, USA*
[45]*Lawrence Berkeley National Laboratory and University of California, Berkeley, California 94720, USA*
[46]*California State University, Fresno, California 93740, USA*
[47]*University of California, Riverside, California 92521, USA*
[48]*Florida State University, Tallahassee, Florida 32306, USA*
[49]*Fermi National Accelerator Laboratory, Batavia, Illinois 60510, USA*
[50]*University of Illinois at Chicago, Chicago, Illinois 60607, USA*
[51]*Northern Illinois University, DeKalb, Illinois 60115, USA*
[52]*Northwestern University, Evanston, Illinois 60208, USA*
[53]*Indiana University, Bloomington, Indiana 47405, USA*
[54]*University of Notre Dame, Notre Dame, Indiana 46556, USA*
[55]*Iowa State University, Ames, Iowa 50011, USA*
[56]*University of Kansas, Lawrence, Kansas 66045, USA*
[57]*Kansas State University, Manhattan, Kansas 66506, USA*
[58]*Louisiana Tech University, Ruston, Louisiana 71272, USA*
[59]*University of Maryland, College Park, Maryland 20742, USA*
[60]*Boston University, Boston, Massachusetts 02215, USA*
[61]*Northeastern University, Boston, Massachusetts 02115, USA*
[62]*University of Michigan, Ann Arbor, Michigan 48109, USA*
[63]*Michigan State University, East Lansing, Michigan 48824, USA*
[64]*University of Mississippi, University, Mississippi 38677, USA*
[65]*University of Nebraska, Lincoln, Nebraska 68588, USA*
[66]*Princeton University, Princeton, New Jersey 08544, USA*
[67]*Columbia University, New York, New York 10027, USA*
[68]*University of Rochester, Rochester, New York 14627, USA*
[69]*State University of New York, Stony Brook, New York 11794, USA*
[70]*Brookhaven National Laboratory, Upton, New York 11973, USA*
[71]*Langston University, Langston, Oklahoma 73050, USA*
[72]*University of Oklahoma, Norman, Oklahoma 73019, USA*
[73]*Brown University, Providence, Rhode Island 02912, USA*
[74]*University of Texas, Arlington, Texas 76019, USA*
[75]*Southern Methodist University, Dallas, Texas 75275, USA*
[76]*Rice University, Houston, Texas 77005, USA*
[77]*University of Virginia, Charlottesville, Virginia 22901, USA*
[78]*University of Washington, Seattle, Washington 98195, USA*

Using the data accumulated in 2002–2004 with the D0 detector in proton-antiproton collisions at the Fermilab Tevatron collider with a center-of-mass energy of 1.96 TeV, the branching fractions of the decays $B \rightarrow \bar{D}_1^0(2420)\mu^+\nu_\mu X$ and $B \rightarrow \bar{D}_2^{*0}(2460)\mu^+\nu_\mu X$ and their ratio have been measured: $\mathcal{B}(\bar{b} \rightarrow B) \times \mathcal{B}(B \rightarrow \bar{D}_1^0\mu^+\nu_\mu X) \times \mathcal{B}(\bar{D}_1^0 \rightarrow D^{*-}\pi^+) = [0.087 \pm 0.007(\text{stat}) \pm 0.014(\text{syst})]\%$; $\mathcal{B}(\bar{b} \rightarrow B) \times \mathcal{B}(B \rightarrow \bar{D}_2^{*0}\mu^+\nu_\mu X) \times \mathcal{B}(\bar{D}_2^{*0} \rightarrow D^{*-}\pi^+) = [0.035 \pm 0.007(\text{stat}) \pm 0.008(\text{syst})]\%$ and $[\mathcal{B}(B \rightarrow \bar{D}_2^{*0}\mu^+\nu_\mu X) \times \mathcal{B}(\bar{D}_2^{*0} \rightarrow D^{*-}\pi^+)]/[\mathcal{B}(B \rightarrow \bar{D}_1^0\mu^+\nu_\mu X) \times \mathcal{B}(\bar{D}_1^0 \rightarrow D^{*-}\pi^+)] = 0.39 \pm 0.09(\text{stat}) \pm 0.12(\text{syst})$, where the charge conjugated states are always implied.

This Letter describes our investigation of the properties of semileptonic decays of $B$ mesons to orbitally excited states of the $D$ meson that have small decay widths. In the simplest case, these states consist of a charm quark and a light quark in a state with orbital angular momentum equal to one. In the limit of a large charm quark mass $m_c \gg \Lambda_{QCD}$, one doublet of states with $j = 3/2$ $(D_1, D_2^*)$ and another doublet with $j = 1/2$ $(D_0^*, D_1')$ are predicted to exist, where the angular momentum $j$ is the sum of the light quark spin and orbital angular momentum. Conservation of parity and angular momentum restricts the final states that are allowed in the decays of these particles collectively known as $D^{**}$ mesons. The states that decay through a $D$ wave, $D_1$ and $D_2^*$, are expected to have small decay widths, $O(10 \text{ MeV}/c^2)$, while the states that decay through an $S$ wave, $D_0^*$ and $D_1'$, are expected to be broad, $O(100 \text{ MeV}/c^2)$.

The ratio $R$ of the semileptonic branching fractions of the $B$ meson to $D_1$ and $D_2^*$:

$$R = \frac{\mathcal{B}(B \to D_2^* \ell \bar{\nu})}{\mathcal{B}(B \to D_1 \ell \bar{\nu})}, \quad (1)$$

is one of the least model-dependent predictions of heavy quark effective theory (HQET) [1] for these states. This ratio is expected to be equal to 1.6 in the infinite charm quark mass limit [2], but it can have a lower value once $O(1/m_c)$ corrections are taken into account [3,4]. Together with the measurement of the corresponding ratio $R_\pi$ for the nonleptonic decays $B \to D^{**} \pi$, determination of $R$ will provide important tests of HQET and factorization of the nonleptonic decays [3].

The narrow $D^{**}$ mesons have been previously studied by several experiments, most recently at Belle [5] where the ratio $R_\pi$ was measured. The semileptonic decay fractions of $B$ mesons to $D^{**}$ mesons were reported previously by the ARGUS [6], CLEO [7], OPAL [8], ALEPH [9], and DELPHI (as preliminary) [10] Collaborations, with only the latter measuring the fraction of $B \to D_2^* \ell \bar{\nu}$ and the others setting upper limits for this decay mode.

The data set used for this analysis corresponds to $\approx$ 460 pb$^{-1}$ of integrated luminosity accumulated by the D0 detector between April 2002 and September 2004 in proton-antiproton collisions at the Fermilab Tevatron collider at center-of-mass energy 1.96 TeV. The D0 detector has a central tracking system consisting of a silicon microstrip tracker (SMT) and a central fiber tracker (CFT) [11]. Both are located within a 2 T superconducting solenoidal magnet and have designs optimized for tracking and vertexing for $|\eta| < 3$ and $|\eta| < 2.5$ [12], respectively. The SMT has a six-barrel longitudinal structure, each with a set of four layers arranged axially around the beam pipe, and interspersed with 16 radial disks. Silicon sensors have typical strip pitch of 50–150 $\mu$m. The CFT has eight thin coaxial barrels, each supporting two doublets of overlapping scintillating fibers of 0.835 mm diameter. The next

layer of detection involves a preshower constructed of scintillator strips and a liquid-argon/uranium calorimeter. An outer muon system, covering $|\eta| < 2$, consists of a layer of tracking detectors and scintillation trigger counters in front of 1.8 T iron toroids, followed by two similar layers after the toroids [13]. A suite of single-muon online triggers was used to record the data set while offline only information from the muon and tracking systems was used in this analysis.

Production of narrow $D^{**}$ mesons in $B \to D^{*-}\pi^+\mu^+\nu_\mu X$ decay manifests itself as resonance peaks in the $D^{*-}\pi^+$ [14] invariant mass spectrum. To perform the measurement, the semileptonic branching fractions of $B$ mesons to the $D^{**}$ mesons were normalized to the $B \to D^{*-}\mu^+\nu_\mu X$ process.

Initially, a sample of $\mu^\pm \bar{D}^0$ candidates was selected by requiring a muon with transverse momentum $p_T^\mu > 2$ GeV$/c$ and $|\eta^\mu| < 2$. $\bar{D}^0$ mesons were reconstructed through their decays into $K^+\pi^-$. Two tracks with $p_T > 0.7$ GeV$/c$ and $|\eta| < 2$ were required to belong to the same jet and to form a common $\bar{D}^0$ vertex following the procedure described in detail in Ref. [15]. To increase the signal yield, the event selections of Ref. [15] were relaxed by removing the explicit requirement that the $p_T$ of the $\bar{D}^0$ exceeds 5 GeV$/c$. In total $216\,870 \pm 1280(\text{stat})\mu^+\bar{D}^0$ candidates were found.

$D^{*-}$ candidates were selected through their decays into $\bar{D}^0\pi^-$ by requiring an additional track with $p_T > 0.18$ GeV$/c$ and the charge opposite to that of the muon. The mass difference $\Delta M = M(K\pi\pi) - M(K\pi)$ for all such tracks with assigned pion mass is shown in Fig. 1 for events with $1.75 < M(K\pi) < 1.95$ GeV$/c^2$. The signal was described as the sum of two Gaussian functions and
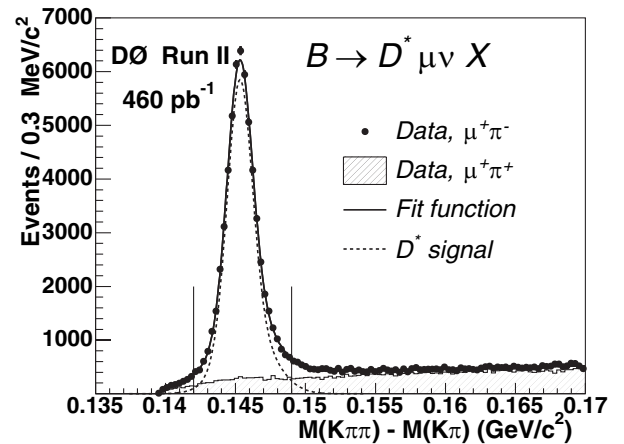


FIG. 1. Distribution of the mass difference $M(K\pi\pi) - M(K\pi)$ for events with $1.75 < M(K\pi) < 1.95$ GeV$/c^2$. The fit function describes the signal as the sum of two Gaussian functions and the background as the sum of exponential and first-order polynomial functions. The signal contribution is also shown separately. The hatched histogram corresponds to the same-sign combination of the muon and pion charges.

the background as the sum of exponential and first-order polynomial functions. The total number of $D^{*-}$ candidates in the peak is $55\,450 \pm 280$(stat) and is defined as the number of signal events in the mass difference window between 0.142 and 0.149 GeV/$c^2$.

To select a sample of $B \to D^{*-} \mu^+ \nu_\mu X$ decays used later both for the signal search and for the normalization, $B$ candidates were defined using the $\mu^+$ and $D^{*-}$ particles. All tracks used for the reconstruction of the $B$ candidate had to have at least two SMT and six CFT hits. The decay length of the $B$ meson, defined in the axial plane [16] as the distance between the primary vertex [15] and the $B$ meson vertex, was restricted to be less than 1 cm, the uncertainty on the $B$-vertex axial position had to be less than 0.5 mm, and the $\chi^2$ of the $B$-vertex fit had to be less than 25 for 3 degrees of freedom. The significance of the decay length in the axial plane and the proper decay length of the $B$ meson [15] were required to exceed 3.0 and 0.25 mm, respectively. The significance is defined as the ratio of the decay length to its uncertainty. The last selection, more stringent than in Ref. [15], reduces the $c\bar{c}$ contamination in the $\mu^+ D^{*-}$ sample to less than 1%. After these selections, the total number of $D^{*-}$ candidates in the invariant mass difference peak is $N_{D^*} = 31160 \pm 230$(stat).

$D^{**}$ decays can be selected by combining the $D^*$ candidates with an additional track with assigned pion mass. The track was required to have a charge opposite to that of the $D^*$, $p_T > 0.3$ GeV/$c$, and at least two SMT and six CFT hits. Pions from the $D^{**}$ decay can also be selected by their topology since the corresponding track originates from the $B$ vertex rather than from the primary vertex. The impact parameters (IP) in the axial plane with respect to the primary and with respect to the $B$ vertex were determined for each track. In order to select tracks belonging to the $B$ vertex, the ratio of IP significances of the track for the primary and $B$ vertices was required to be greater than four and the IP significance with respect to the primary vertex
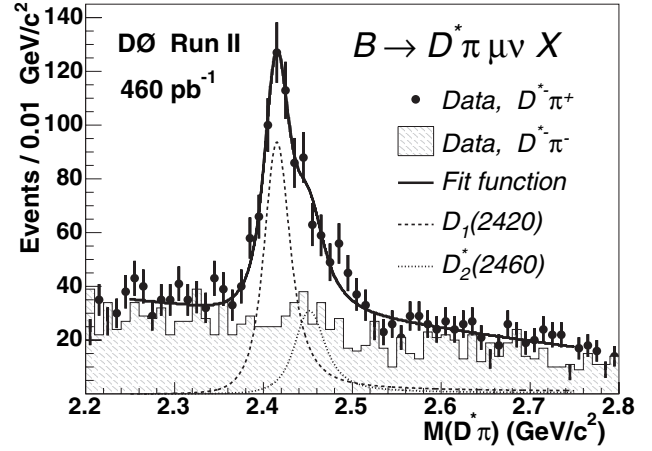


FIG. 2.   The invariant mass $M(D^* \pi)$. Event selection is described in the text. The points correspond to the $D^* \pi$ combinations with opposite charges, and the hatched histogram corresponds to the same-charge combinations. The distribution was fit with a sum of two relativistic Breit-Wigner functions corresponding to two narrow $D^{**}$ states and a second-order polynomial describing the background. The contributions of $D_1^0$ and $D_2^{*0}$ to the fit are shown separately.

was required to be greater than one. The IP significance is defined as the ratio of the impact parameter to its uncertainty.

The $D^{**}$ invariant mass distribution after all selections is shown in Fig. 2 where the $D^*$ mass from the Particle Data Group (PDG) [17] has been used as a mass constraint. The observed mass peak can be interpreted as two merged narrow $D^{**}$ states, $D_1^0$ and $D_2^{*0}$.

The distribution was fit using a sum of two relativistic Breit-Wigner functions $G_{D_1}$ and $G_{D_2^*}$, corresponding to the two narrow $D^{**}$ states with the numbers of events $N_{D_1}$ and $N_{D_2^*}$, respectively, and a second-order polynomial $f_b$ describing the background, see Eq. (2).

$$f(x) = N_{D_1} G_{D_1} + N_{D_2^*} G_{D_2^*} + f_b(x); \qquad G_i = \frac{M_i \Gamma(x)}{(x^2 - M_i^2)^2 + M_i^2 \Gamma(x)^2} \otimes \mathrm{Res}_i;$$

$$\Gamma(x) = \Gamma_i \frac{M_i}{x} \left(\frac{k}{k_0}\right)^{2L+1} F^{(L)}(k, k_0); \qquad F^{(2)}(k, k_0) = \frac{9 + 3(k_0 z)^2 + (k_0 z)^4}{9 + 3(kz)^2 + (kz)^4}. \tag{2}$$

In the formulas above, $x$ is the $D^* \pi$ invariant mass and $M_i$ and $\Gamma_i$ are the mass and width of the corresponding resonance. The variables $k$ and $k_0$ are the pion three-momenta in the $D^{**}$ rest frame when the $D^{**}$ has a four-momentum-squared equal to $x^2$ and $M_i^2$, respectively. $F^{(2)}(k, k_0)$ is the Blatt-Weisskopf form factor for $D$ wave ($L = 2$) decays of $D^{**}$ mesons [18], and $z = 1.6$ (GeV/$c$)$^{-1}$ is a hadron scale corresponding to the case of the charm quark. $\mathrm{Res}_i$ is the mass resolution function described by two Gaussian functions with the parametrization determined from Monte Carlo (MC) simulations. The second Gaussian describing the resolution

corresponded to 28% of events and was wider by a factor of 2.2 than the first one. The standard D0 simulation chain included the EVTGEN [19] generator interfaced to PYTHIA [20] and followed by full GEANT [21] modeling of the detector response and event reconstruction. The MC resolution was scaled up by 20% to account for the difference between the data and the MC, where the scaling factor was estimated by comparing the $D^*$ mass resolution in the data and MC. The mass resolution used for the fit (sigma of the first Gaussian in the resolution function) was 8.2 MeV/$c^2$ for $D_1^0$ and 9.4 MeV/$c^2$ for $D_2^{*0}$ after the scaling.

The parameters of the background function were determined by fitting the distribution of the same-charge combinations, fixing the function shape parameters, and allowing the overall normalization of the background to float in the mass fit. The mass difference between $D_1^0$ and $D_2^{*0}$ and the widths of $D_1^0$ and $D_2^{*0}$ were fixed in the fit using their corresponding values from the PDG [17]: $36.7 \pm 2.7$ MeV/$c^2$, $18.9^{+4.6}_{-3.5}$ MeV/$c^2$, $23 \pm 5$ MeV/$c^2$. The numbers of events in the two narrow states derived from the fit, $N_{D_1} = 467 \pm 39$(stat) and $N_{D_2^*} = 176 \pm 37$(stat),

were used to determine the total number of events $N_{D^{**}} = 643 \pm 38$(stat), and the ratio $N_{D_2^*}/N_{D_1} = 0.378 \pm 0.086$(stat), where the uncertainties take into account correlation between the variables. The $\chi^2$ of the fit at the minimum is 46.9 for 46 degrees of freedom.

The branching fraction for the decays $B \to \bar{D}^{**} \mu^+ \nu_\mu X$ can be determined by normalization to the known value of the branching fraction $\mathcal{B}(\bar{b} \to D^{*-} \ell^+ \nu X) = (2.75 \pm 0.19)\%$ [18]. The following two formulas were used for the calculations:

$$\mathcal{B}(\bar{b} \to B) \times \mathcal{B}(B \to \bar{D}^{**} \mu^+ \nu_\mu X) \times \mathcal{B}(\bar{D}^{**} \to D^{*-} \pi^+) = \mathcal{B}(\bar{b} \to D^{*-} \ell^+ \nu X) \frac{N_{D^{**}}}{N_{D^*}} \frac{1}{\epsilon_{D^{**}}};$$

$$\frac{\mathcal{B}(B \to \bar{D}_2^{*0} \mu^+ \nu_\mu X) \times \mathcal{B}(\bar{D}_2^{*0} \to D^{*-} \pi^+)}{\mathcal{B}(B \to \bar{D}_1^0 \mu^+ \nu_\mu X) \times \mathcal{B}(\bar{D}_1^0 \to D^{*-} \pi^+)} = \frac{N_{D_2^*}}{N_{D_1}} \frac{\epsilon_{D_1}}{\epsilon_{D_2^*}}.$$

$N_{D^{**}}$ and $N_{D^*}$ are the numbers of $D^{**}$ and $D^*$ candidates as defined above. The $D^{**}$ notation stands for $D_1^0$ or $D_2^{*0}$ or both of them, $(D_1^0, D_2^{*0})$. $\epsilon_{D^{**}}$ is the efficiency to reconstruct the charged pion from the $D^{**}$ decay determined from the MC and equal to $[47.2 \pm 1.0$(stat)$]\%$ for the $D_1^0$ meson and $[45.4 \pm 1.2$(stat)$]\%$ for the $D_2^{*0}$ meson. Contributions from $B_s$ mesons, $\Lambda_b$ baryons, and $B \to D_{(s)}^{(*)} D^{*-} X$ decays to the sample were found to be small and have been neglected [16].

The relative systematic uncertainties on the branching fractions and of their ratio are summarized in Table I. The contribution due to uncertainty in $\mathcal{B}(\bar{b} \to D^{*-} \ell^+ \nu X)$ was determined from the uncertainty on this branching fraction. The systematic uncertainty caused by the MC mass resolution was estimated by varying the resolution by $\pm 20\%$. Contributions due to limited knowledge of the $D^{**}$ masses and widths were computed by refitting the mass distribution after varying these parameters within their uncertainties. The systematic uncertainty due to efficiency modeling accounts for the variation caused by a possible mismatch

between the $p_T$ spectra of reconstructed particles in the data and MC.

There are predictions and possibly observations [6] of a wide resonance $\bar{D}_1'^0$ with a mass of 2430 MeV/$c^2$ and a width of 380 MeV/$c^2$ predominantly decaying to $D^{*-} \pi^+$. This resonance is not apparent in our data, and it was not used in the fits. The systematic uncertainty caused by a possible contribution of this resonance was evaluated allowing for another Breit-Wigner function in the fit, with the mass and width fixed to the wide resonance parameters.

Any interference effects between the $D_1^0$ and $D_2^{*0}$ must average to zero after integration over all angles under the assumption of equal acceptances. The validity of this assumption has been checked and the corresponding uncertainty assigned. The systematic uncertainty due to the fitting procedure was estimated by varying the functions describing the backgrounds for the $D^*$ and $D^{**}$ mass distributions and also the function describing the $D^*$ mass peak. The total systematic uncertainty was found by summing all the above sources in quadrature.

TABLE I. Relative systematic uncertainties on the semileptonic branching fraction to both narrow states, $\mathcal{B}_{D^{**}}$; the semileptonic branching fractions to $D_1^0$ and to $D_2^{*0}$, $\mathcal{B}_{D_1}$ and $\mathcal{B}_{D_2^*}$; and their ratio $\mathcal{B}_{D_2^*}/\mathcal{B}_{D_1}$.

| Source | $\mathcal{B}_{D^{**}}$ | $\mathcal{B}_{D_1}$ | $\mathcal{B}_{D_2^*}$ | $\mathcal{B}_{D_2^*}/\mathcal{B}_{D_1}$ |
|---|---|---|---|---|
| $\mathcal{B}(\bar{b} \to D^{*-} \ell^+ \nu X)$ | 7% | 7% | 7% | — |
| Mass resolution | 2% | 4% | 5% | 8% |
| $\Gamma_{D_1}$ | 3% | 11% | 16% | 24% |
| $\Gamma_{D_2^*}$ | 2% | 2% | 11% | 13% |
| $\Delta M$ | 1% | 3% | 6% | 9% |
| MC statistics | 2% | 2% | 2% | 3% |
| $\epsilon_{D^{**}}$ modeling | 3% | 3% | 3% | 2% |
| Wide resonance | 5% | 5% | 5% | 2% |
| Interference effects | 2% | 2% | 2% | 2% |
| $D^*$ fit and $D^{**}$ bkg fit | 4% | 4% | 4% | 1% |
| Total uncertainty | 12% | 16% | 24% | 30% |

Using the numbers defined above, the semileptonic branching fractions of $B$ mesons to $D^{**}$ mesons and their ratio are:

$$\mathcal{B}(\bar{b} \to B) \times \mathcal{B}[B \to (\bar{D}_1^0, \bar{D}_2^{*0})\mu^+\nu_\mu X] \times \mathcal{B}[(\bar{D}_1^0, \bar{D}_2^{*0}) \to D^{*-}\pi^+] = [0.122 \pm 0.007(\text{stat}) \pm 0.015(\text{syst})]\%;$$

$$\mathcal{B}(\bar{b} \to B) \times \mathcal{B}(B \to \bar{D}_1^0\mu^+\nu_\mu X) \times \mathcal{B}(\bar{D}_1^0 \to D^{*-}\pi^+) = [0.087 \pm 0.007(\text{stat}) \pm 0.014(\text{syst})]\%;$$

$$\mathcal{B}(\bar{b} \to B) \times \mathcal{B}(B \to \bar{D}_2^{*0}\mu^+\nu_\mu X) \times \mathcal{B}(\bar{D}_2^{*0} \to D^{*-}\pi^+) = [0.035 \pm 0.007(\text{stat}) \pm 0.008(\text{syst})]\%;$$

$$\frac{\mathcal{B}(B \to \bar{D}_2^{*0}\mu^+\nu_\mu X) \times \mathcal{B}(\bar{D}_2^{*0} \to D^{*-}\pi^+)}{\mathcal{B}(B \to \bar{D}_1^0\mu^+\nu_\mu X) \times \mathcal{B}(\bar{D}_1^0 \to D^{*-}\pi^+)} = [0.39 \pm 0.09(\text{stat}) \pm 0.12(\text{syst})].$$

Upon using the input $\mathcal{B}(\bar{b} \to B) = (39.7 \pm 1.0)\%$ [17], assuming isospin conservation and that the $D_1$ meson decays only into $D^*\pi$ [22], the branching fraction $\mathcal{B}(B \to \bar{D}_1^0\ell^+\nu X) = (0.33 \pm 0.06)\%$ is determined. It is different from the PDG value, $(0.74 \pm 0.16)\%$ [17], by 2.5 standard deviations. Similarly the branching fraction $\mathcal{B}(B \to \bar{D}_2^{*0}\ell^+\nu X) = (0.44 \pm 0.16)\%$ is determined assuming that $D_2^*$ decays into $D^*\pi$ in $(30 \pm 6)\%$ of the cases [17]. This result is in agreement with the 95% C.L. upper limit 0.65% provided by the PDG.

Using the measured ratio of the branching fractions and the same assumptions for the absolute fractions for $D_1$ and $D_2^*$ as above, the ratio $R = 1.31 \pm 0.29(\text{stat}) \pm 0.47(\text{syst})$ was computed.

In summary, using 460 pb$^{-1}$ of integrated luminosity accumulated with the D0 detector, the semileptonic decays $B \to \bar{D}_1^0\mu^+\nu_\mu X$ and $B \to \bar{D}_2^{*0}\mu^+\nu_\mu X$ have been observed and the branching fractions measured using statistics more than an order of magnitude better than previous measurements [6–10]. This result represents a significant improvement in the knowledge of $B$ branching fractions to orbitally excited $D$ mesons, and the first direct measurement of their ratio.

*Visitor from University of Zurich, Zurich, Switzerland.
[1] N. Isgur and M. B. Wise, Phys. Lett. B **232,** 113 (1989); E. Eichten and B. Hill, Phys. Lett. B **234,** 511 (1990); H. Georgi, Phys. Lett. B **240,** 447 (1990).

[2] V. Morenas, A. Le Yaouanc, L. Oliver, O. Pene, and J.-C. Raynal, Phys. Rev. D **56,** 5668 (1997); Ming-Qiu Huang and Yuan-Ben Dai, Phys. Rev. D **59,** 034018 (1999).

[3] A. K. Leibovich, Z. Ligeti, I. W. Stewart, and M. B. Wise, Phys. Rev. Lett. **78,** 3995 (1997); Phys. Rev. D **57,** 308 (1998).

[4] D. Ebert, R. N. Faustov, and V. O. Galkin, Phys. Rev. D **62,** 014032 (2000).

[5] K. Abe *et al.* (Belle Collaboration), Phys. Rev. D **69,** 112002 (2004).

[6] H. Albrecht *et al.* (ARGUS Collaboration), Z. Phys. C **57,** 533 (1993).

[7] A. Anastassov *et al.* (CLEO Collaboration) Phys. Rev. Lett. **80,** 4127 (1998).

[8] G. Abbiendi *et al.* (OPAL Collaboration), Eur. Phys. J. C **30,** 467 (2003).

[9] D. Buskolic *et al.* (ALEPH Collaboration), Z. Phys. C **73,** 601 (1997).

[10] D. Bloch *et al.* (DELPHI Collaboration), DELPHI Report No. 2000-106-CONF, 2000 (unpublished).

[11] V. Abazov *et al.* (The Upgraded D0 Detector), Nucl. Instrum. Methods Phys. Res., Sect. A (to be published).

[12] The pseudorapidity $\eta$ is defined using the polar angle with respect to the proton beam direction, $\theta$, as $\eta = -\ln[\tan(\theta/2)]$.

[13] V. Abazov *et al.* (The Muon System of the Run II D0 Detector), physics/0503151; S. Abachi *et al.,* Nucl. Instrum. Methods Phys. Res., Sect. A **338,** 185 (1994).

[14] $B$ refers to the $B^0$ and $B^+$ mesons, and charge conjugate states are always implied throughout the Letter.

[15] V. Abazov *et al.* (D0 Collaboration), Phys. Rev. Lett. **94,** 182001 (2005).

[16] Axial plane is defined as a plane transverse to the beam direction.

[17] S. Eidelman *et al.* (Particle Data Group), Phys. Lett. B **592,** 1 (2004).

[18] J. Blatt and V. Weisskopf, *Theoretical Nuclear Physics* (Wiley, New York, 1952), p. 361.

[19] D. J. Lange, Nucl. Instrum. Methods Phys. Res., Sect. A **462,** 152 (2001).

[20] T. Sjöstrand *et al.,* Comput. Phys. Commun. **135,** 238 (2001).

[21] R. Brun *et al.,* CERN Report No. DD/EE/84-1, 1984 (unpublished).

[22] A. V. Manohar and M. B. Wise, *Heavy Quark Physics* (Cambridge University Press, Cambridge, England, 2000), p. 10.